CCFE
CULHAM CENTRE FOR FUSION ENERGY

UK Atomic Energy Authority

UKAEA-CCFE-PR(18)64

Frank Schoofs, Mike Gorley

A route to standardised high heat flux testing: an example for tungsten

A route to standardised high heat flux testing: an example for tungsten

Frank Schoofs, Mike Gorley

This is a preprint of a paper submitted for publication in
Nuclear Materials and Energy

A route to standardised high heat flux testing: an example for tungsten

Frank Schoofs, Mike Gorley

United Kingdom Atomic Energy Authority, Culham Centre for Fusion Energy, Culham Science Centre, Abingdon, Oxon, OX14 3DB, UK

A comprehensive, standardised approach to high heat flux testing of materials is proposed, which allows for standardised data capture and comparison of measurements across global testing sites and setups. A meta-analysis of data for tungsten, with data re-captured in that format, highlights interesting trends with respect to appropriate damage metrics and intrinsic material behaviour.

1. Introduction

Plasma facing materials (PFM) in magnetic confinement fusion reactors are exposed to extremely high heat fluxes (HHF), varying over multiple orders of magnitude, from 1 to 10^4 MW/m^2. Typically, there is a steady-state or cyclic base load, e.g. 1-5 MW/m^2 on the first wall or 5-20 MW/m^2 in the divertor region. Occasional superposed high-heat, transient, incidences caused by ELMs (10^3-10^4 MW/m^2) or vertical displacement events and disruptions (10^2-10^4 MW/m^2) can occur [1,2].

In order to qualify PFMs and their behaviour under these conditions, HHF tests are conducted, with the heat load simulated by electrons [3–5], ions [6,7], plasma [8,9], induction [10] or lasers [11]. These tests are time consuming and testing the entire parameter space is impractical for a single testing site. Worldwide there are several sites that can do HHF testing [1,12,13], but it is therefore important to combine measurements performed on different HHF test beds in order to provide a comprehensive picture of material performance under the wide range of conditions.

In this paper a methodology is presented to ensure that HHF measurements are representative of intrinsic material performance. It also provides a starting point to develop a standardised approach to HHF data collection and analysis. The method is then applied to pure tungsten (W), a leading contender for the DEMO PFM on the first wall and divertor [14].

2. Methodology

2.1 Material definition

Typically, samples are 12x12 mm^2 or 10x10 mm^2. It is important that the samples are significantly larger than the beam spot to avoid edge effects. The sample thickness needs to be at least 5 mm (and preferably 10 mm) to observe bulk properties [9]. The surface needs to be mechanically polished, e.g. by SiC paper and diamond paste, to a defined starting R_a, e.g. 0.1 μm. This ensures that the power absorption, roughness increase and crack initiation due to surface defects are controlled and can be compared across measurements.

We propose that the properties and information outlined in Table 1 are captured for the samples. This ensures traceability and allows researchers to analyse the effect of different intrinsic parameters on the material performance. For alloys or targeted doping experiments, the ‘purity’ category can be expanded or specified.

Table 1: Details of starting materials to be specified when reporting HHF test results.

Material property/identifier	Comments
Supplier	Company & location
Condition	Combination of manufacturing and heat treatments E.g. as-coated, sintered, forged, rolled, stress relieved, recrystallised
Purity	Minimum specified
Density	Actual (measured) or minimum specified
Grain orientation	If anisotropic, specify orientation of test e.g. longitudinal, transversal
Feret diameter (min)	Indication of level of anisotropy or cold work of starting microstructure (optional)
Feret diameter (max)	
Surface roughness	If different from R_a = 0.1 μm

2.2 Reported measurement parameters

Information that needs to be logged for testing conditions is given in Table 2. If the base temperature is not room temperature, the method of heating, e.g. ohmic heating or laser/electron beam pre-rastering, needs to be specified, as this may give rise to secondary effects.

The absorption coefficient assumed to calculate the heat load should be explicitly stated as well, as different labs might use (or have used) different coefficients. For example, electron absorption coefficients of 0.46 [15], 0.55 [16] and 0.6 [17] have historically been quoted for tungsten. In order to compare the values, all the heat loads need to be recalculated to the current most widely accepted value.

Table 2: Experimental HHF testing properties & conditions to be logged.

Testing property	Comment (units if applicable)
Heating method	e.g. electron beam, laser
Base temperature	(°C or K)
Area scanned	e.g. raster scan or not (mm^2)
Beam spot size	(mm)
Absorption coefficient	(-)
Absorbed heat load (power density)	(MW/m^2)
Pulse duration	(ms)
Pulse count	Number of pulses/cycles (-)
Repetition rate	Frequency of pulses (in Hz)
Ion/electron energy	If applicable (eV)
Ion dose	If applicable ($/mm^2$)

2.3 Reported result parameters

Table 3 shows the type of metrics that would ideally be captured following a HHF experiment. As a minimum, the damage category should be stated. The types of damages induced into the materials

can be classified in 6 categories. Below a certain damage threshold, nothing happens. Above that threshold, the surface damage progressively increases from roughening, to cracks, to connected cracks and eventually the material will melt and re-solidify. All of this is a result of the differential thermal expansion between the heated and unheated parts of the sample [18].

It should be noted that these HHF events cause changes in the microstructure. For example, in tungsten, recrystallisation occurs, but to varying degrees depending on the alloying elements and manufacturing method (i.e. the starting microstructure) [2,19–21]. The damage threshold is also strongly dependent on the grain orientation, texture and the degree of recrystallisation, as demonstrated for tungsten [19].

Table 3: Damage metrics to be measured after HHF testing.

Damage metric	**Remarks**
Damage	Possible categories: None / Roughening / Small cracks / Crack network / Cracked, melt droplets / Surface melting
Recrystallised depth	If applicable
Surface roughness	Record R_a over 1x1 mm^2 or entire spot if smaller
Crack distance	Record minimum and maximum of inter-crack distance
Crack width	Record maximum and average surface crack width
Crack depth	Record maximum and average depth

3. Results for tungsten

Data for tungsten were collected from publications from different facilities, namely JUDITH I and II [16,18,19], HHFTF [17,22], EMS-60 [15,23,24], JEBIS [25–27], QSPA-T [28,29], JET NBI test bed [30] and SNU-(T)HLT [21]. This resulted in a total of 229 measurement points with reported damage. All electron beam experiments have been recalculated to use an absorption coefficient of 0.55.

From Figure 1, it is clear that most of the experiments have been performed with the tungsten at room temperature. It should be noted that the anticipated operating temperature under normal DEMO conditions is approximately 300-550 °C for the first wall and 150-250 °C for the divertor [31].

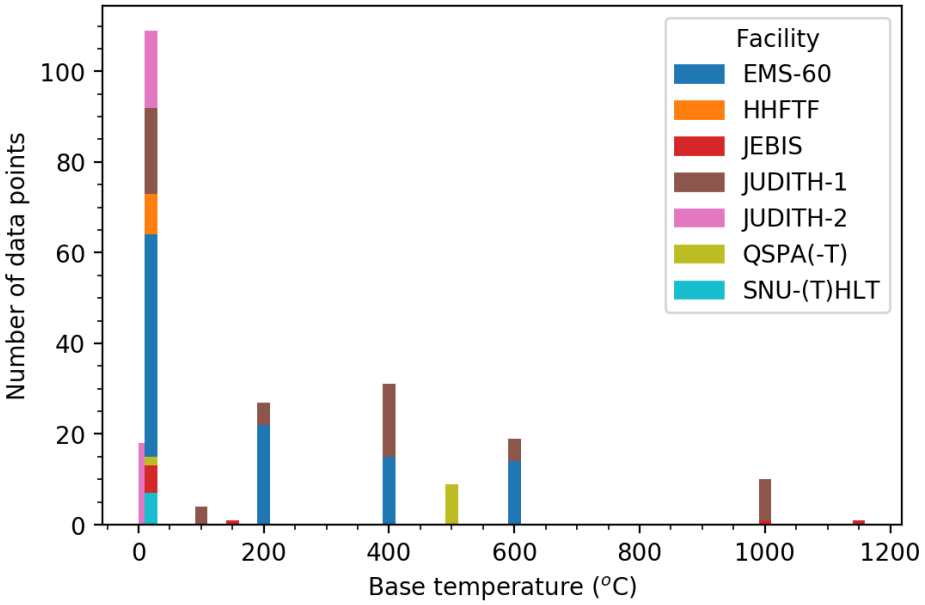

Figure 1: Number of HHF tests with respect the tungsten base temperature at different facilities.

Typical metrics that are used to describe HHF tests are:

a) the absorbed power density on the sample (W/m^2).
b) the absorbed energy density per pulse on the sample (J/m^2).
c) the total energy delivered to the sample (J/m^2), i.e. the absorbed energy density per pulse multiplied by number of pulses.
d) a "heat flux factor" ($W\ s^{0.5}/m^2$), defined as the heat load times the square root of the pulse duration [32].

Figures 2a, 2b, 2c and 2d show the respective maps of these metrics against the base temperature of the tungsten for all data points. It is clear that the absorbed power density gives a reasonable separation of thresholds for various failure modes, which are absent in the other metrics.

It appears that the threshold for the onset of cracking is strongly temperature dependent. At room temperature, it appears to be around ~10 MW/m^2, but this rises to 300-400 MW/m^2 above 200 °C. Above ~800 MW/m^2 surface melting occurs, regardless of the base temperature.

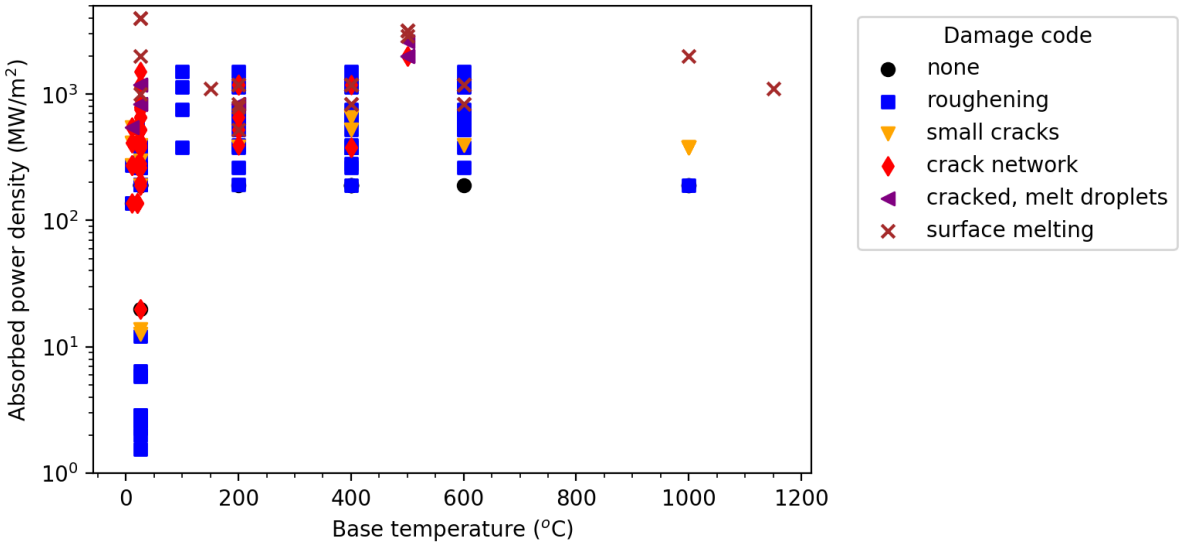
Absorbed power density (MW/m^2)
10^0
10^1
10^2
10^3
0
200
400
600
800
1000
1200
Base temperature (^{o}C)
Damage code
none
roughening
small cracks
crack network
cracked, melt droplets
surface melting

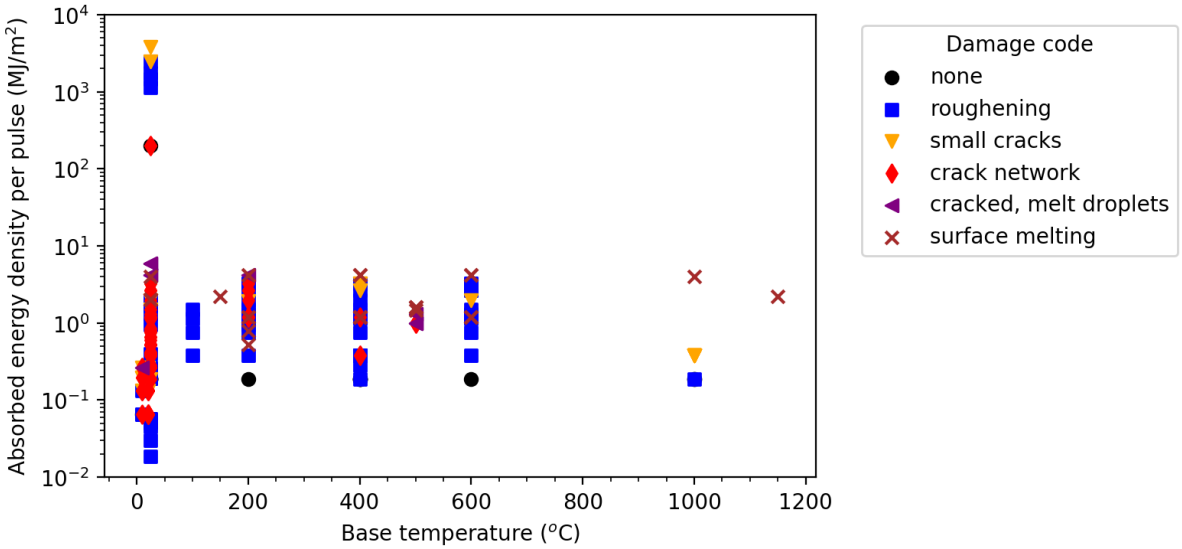
Absorbed energy density per pulse (MJ/m^2)
10^{-2}
10^{-1}
10^0
10^1
10^2
10^3
10^4
0
200
400
600
800
1000
1200
Base temperature (^{o}C)
Damage code
none
roughening
small cracks
crack network
cracked, melt droplets
surface melting

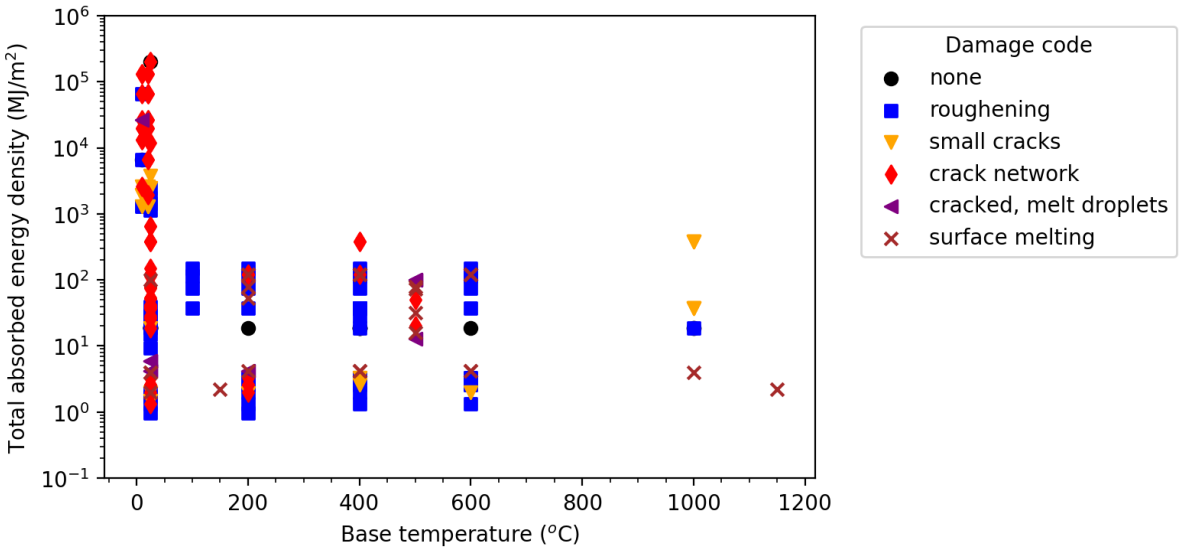
Total absorbed energy density (MJ/m^2)
10^{-1}
10^0
10^1
10^2
10^3
10^4
10^5
10^6
0
200
400
600
800
1000
1200
Base temperature (^{o}C)
Damage code
none
roughening
small cracks
crack network
cracked, melt droplets
surface melting

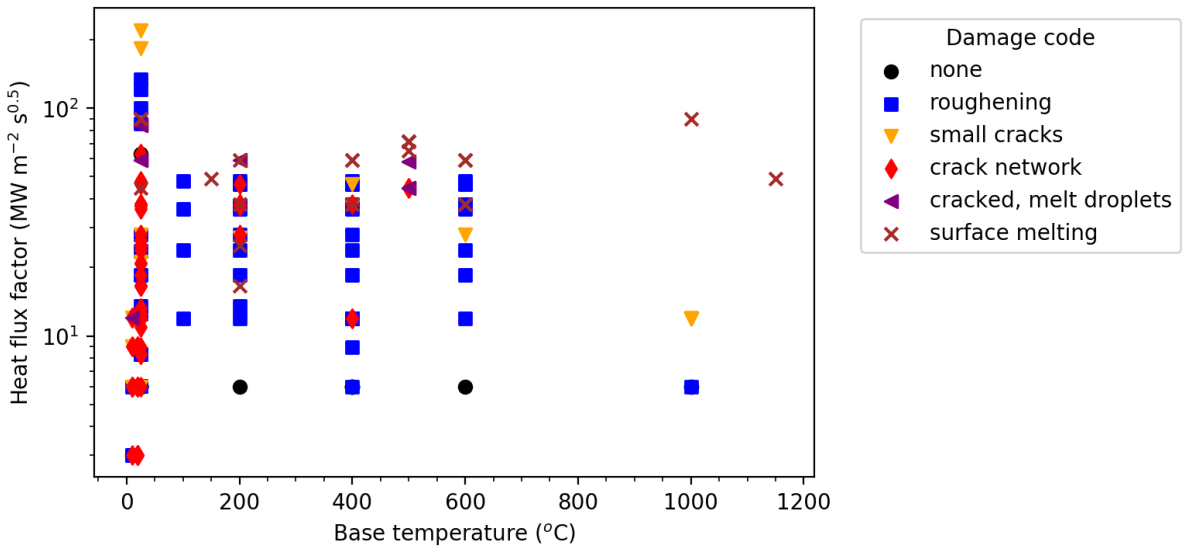

Figure 2: (a) Absorbed power density, (b) absorbed energy density per pulse, (c) total absorbed energy density and (d) heat flux factor versus base temperature, showing the different reported damage codes for each experiment.

In a limited number of references, the peak surface temperature observed during the HHF experiment is also reported [17,21,22,30]. All of these experiments start from tungsten at room temperature. It should be noted that the peak temperature depends on the W thickness, sample geometry and cooling method. Figure 3 shows these temperatures against the absorbed energy density per pulse. All data points are included for comparison, showing a wide variation between 1000 °C and 2000 °C. The simulations show a steeper temperature increase with increasing energy density than the experimental values.

In any case, this means there will be significant recrystallisation in the tungsten – which has also been quantified for a number of HHF experiments [21,25,26,29]. Figure 4 shows the recrystallised depth of the tungsten versus the total energy absorbed during the HHF experiment.

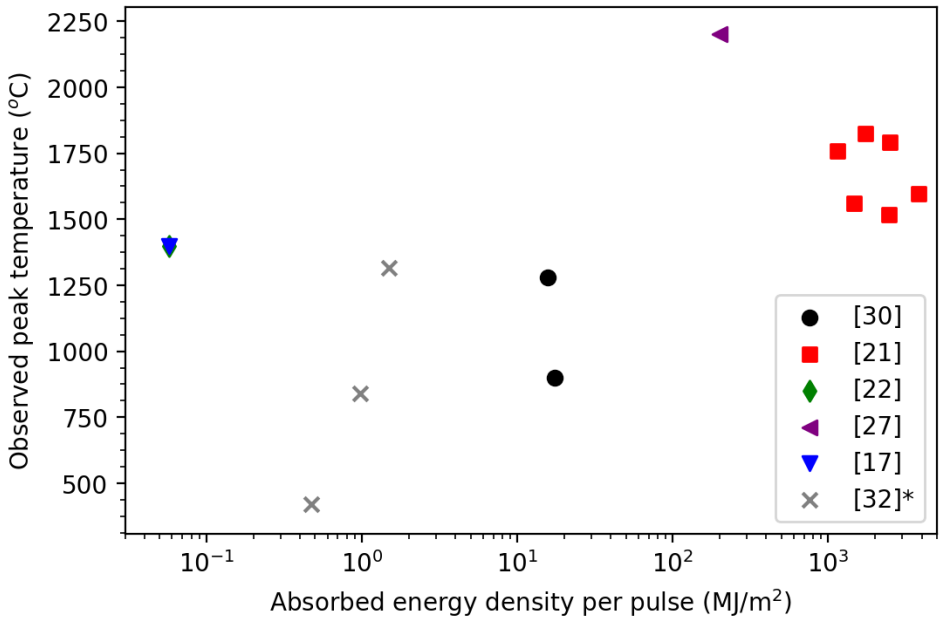

*Figure 3: Observed peak temperature of the tungsten during HHF experiments for different absorbed pulse energies. All experiments started at room temperature. The reference marked with a * indicates simulated values.*

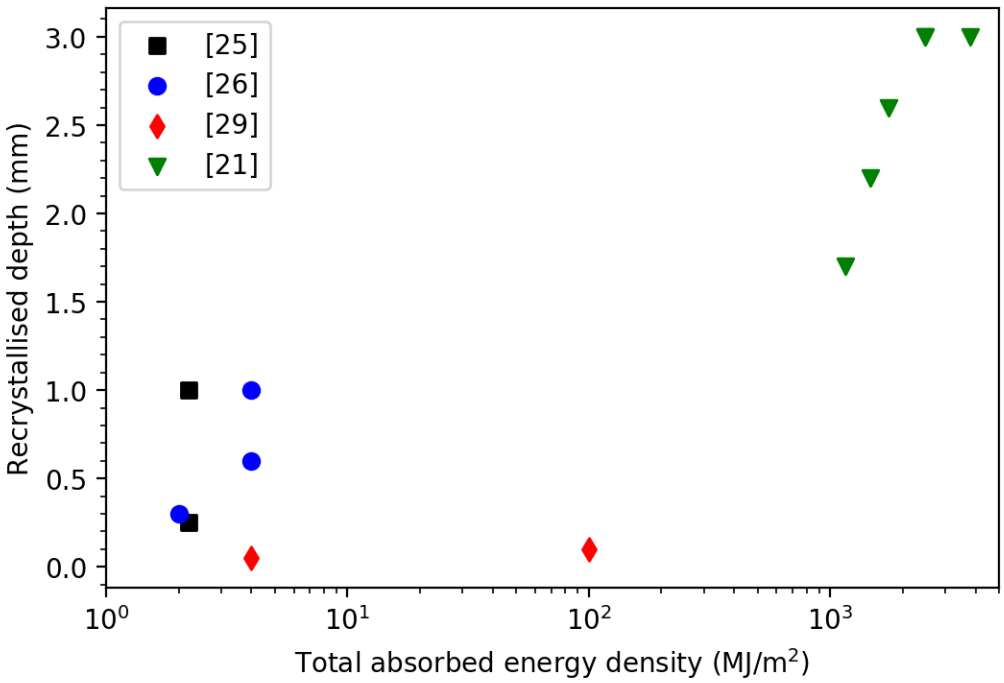

Figure 4: Observed recrystallised depth versus the total absorbed energy density during the HHF experiment.

4. Conclusions

In conclusion, we have proposed an outline of a standardised measurement and data capture method for high heat flux experiments, which allow comparison of data captured at different testing sites. Such a comparison was done for pure tungsten on data from several HHF test beds. The absorbed power density versus base temperature was shown to be a good indicator for damage thresholds. Observed peak temperatures vary from 1200 to 2000 °C, which result in recrystallisation across the depth of the sample, up to 3 mm from the surface. This will have a significant effect on the mechanical properties of the tungsten and its response to stresses inside the plasma facing components.

5. Acknowledgments

F. S. would like to thank M. Wirtz, T. Loewenhoff (FZJ), X. Liu, Y. Lian (SWIP), S. Kanpara (IPR) and G. H. Kim (SNU) for their guidance and support in compiling the methodology and for providing data.

This work has been carried out within the framework of the EUROfusion Consortium and has received funding from the Euratom research and training programme 2014-2018 under grant agreement No 633053 and from the RCUK Energy Programme [grant number EP/I501045]. To obtain further information on the data and models underlying this paper please contact PublicationsManager@ccfe.ac.uk. The views and opinions expressed herein do not necessarily reflect those of the European Commission.

6. References

[1] T. Hirai, K. Ezato, P. Majerus, ITER Relevant High Heat Flux Testing on Plasma Facing Surfaces, Mater. Trans. 46 (2005) 412–424. doi:10.2320/matertrans.46.412.

[2] M. Wirtz, I. Uytdenhouwen, V. Barabash, F. Escourbiac, T. Hirai, J. Linke, T. Loewenhoff, S. Panayotis, G. Pintsuk, Material properties and their influence on the behaviour of tungsten as

plasma facing material, Nucl. Fusion. 57 (2017) 66018. doi:10.1088/1741-4326/aa6938.

[3] P. Majerus, R. Duwe, T. Hirai, W. Kühnlein, J. Linke, M. Rödig, The new electron beam test facility JUDITH II for high heat flux experiments on plasma facing components, Fusion Eng. Des. 75 (2005) 365–369. doi:10.1016/j.fusengdes.2005.06.058.

[4] X. Liu, Y. Lian, Z. Xu, J. Chen, L. Chen, Q. Wang, Progress of High Heat Flux Component Manufacture and Heat Load Experiments in China, in: Proc. 24th IAEA Fusion Energy Conf., San Diego, CA, USA, 2012: p. 7.

[5] J. Prokupek, K. Samec, R. Jílek, P. Gavila, S. Neufuss, S. Entler, HELCZA—High heat flux test facility for testing ITER EU first wall components, Fusion Eng. Des. 124 (2017) 187–190. doi:10.1016/j.fusengdes.2017.03.059.

[6] H. Greuner, B. Boeswirth, J. Boscary, P. McNeely, High heat flux facility GLADIS: Operational characteristics and results of W7-X pre-series target tests, J. Nucl. Mater. 367 (2007) 1444–1448. doi:10.1016/j.jnucmat.2007.04.004.

[7] D. Nicolai, P. Chaumet, O. Neubauer, R. Uhlemann, New options for material testing at the material ion beam test facility MARION, Fusion Eng. Des. 88 (2013) 2506–2509. doi:10.1016/j.fusengdes.2013.02.132.

[8] A. Zhitlukhin, N. Klimov, I. Landman, J. Linke, A. Loarte, M. Merola, V. Podkovyrov, G. Federici, B. Bazylev, S. Pestchanyi, V. Safronov, T. Hirai, V. Maynashev, V. Levashov, A. Muzichenko, Effects of ELMs on ITER divertor armour materials, J. Nucl. Mater. 363–365 (2007) 301–307. doi:10.1016/j.jnucmat.2007.01.027.

[9] G.G. Van Eden, T.W. Morgan, H.J. Van Der Meiden, J. Matejicek, T. Chraska, M. Wirtz, G. De Temmerman, The effect of high-flux H plasma exposure with simultaneous transient heat loads on tungsten surface damage and power handling, Nucl. Fusion. 54 (2014) 123010. doi:10.1088/0029-5515/54/12/123010.

[10] D. Hancock, M. Porton, C.D. Hardie, B. Edwards, R. Bamber, K. Nicholls, A Low Cost High Performance Test Facility for Evaluating Advanced High Heat Flux Concepts, in: Technol. Fusion Energy, Philadelphia, PA, 2016.

[11] A. Huber, A. Arakcheev, G. Sergienko, I. Steudel, M. Wirtz, A. V Burdakov, J.W. Coenen, A. Kreter, J. Linke, P. Mertens, V. Philipps, G. Pintsuk, M. Reinhart, U. Samm, A. Shoshin, B. Schweer, B. Unterberg, M. Zlobinski, Investigation of the impact of transient heat loads applied by laser irradiation on ITER-grade tungsten, Phys. Scr. T159 (2014) 14005. doi:10.1088/0031-8949/2014/T159/014005.

[12] M. Rödig, M. Akiba, P. Chappuis, R. Duwe, M. Febvre, A. Gervash, J. Linke, N. Litounovsky, S. Suzuki, B. Wiechers, D.. Youchison, Comparison of electron beam test facilities for testing of high heat flux components, Fusion Eng. Des. 51–52 (2000) 715–722. doi:10.1016/S0920-3796(00)00219-2.

[13] C. Linsmeier, B. Unterberg, J.W. Coenen, R.P. Doerner, H. Greuner, A. Kreter, J. Linke, H. Maier, Material testing facilities and programs for plasma-facing component testing, Nucl. Fusion. 57 (2017) 92012. doi:10.1088/1741-4326/aa4feb.

[14] D. Stork, P. Agostini, J.-L. Boutard, D. Buckthorpe, E. Diegele, S.L. Dudarev, C. English, G. Federici, M.R. Gilbert, S. Gonzalez, A. Ibarra, C. Linsmeier, A.L. Puma, G. Marbach, L.W. Packer, B. Raj, M. Rieth, M.Q. Tran, D.J. Ward, S.J. Zinkle, Materials R&D for a timely DEMO: Key findings and recommendations of the EU Roadmap Materials Assessment Group, Fusion Eng. Des. 89 (2014) 1586–1594. doi:10.1016/j.fusengdes.2013.11.007.

[15] Y. Lian, X. Liu, Z. Cheng, J. Wang, J. Song, Y. Yu, J. Chen, Thermal shock performance of CVD tungsten coating at elevated temperatures, J. Nucl. Mater. 455 (2014) 371–375. doi:10.1016/j.jnucmat.2014.07.021.

[16] M. Wirtz, J. Linke, T. Loewenhoff, G. Pintsuk, I. Uytdenhouwen, Thermal shock tests to qualify different tungsten grades as plasma facing material, Phys. Scr. T167 (2016) 14015. doi:10.1088/0031-8949/T167/1/014015.

[17] S. Kanpara, S. Khirwadkar, S. Belsare, K. Bhope, R. Swamy, Y. Patil, P. Mokariya, N. Patel, T. Patel, K. Galodiya, Fabrication of Tungsten & Tungsten Alloy and its High Heat Load Testing for Fusion Applications, Mater. Today Proc. 3 (2016) 3055–3063. doi:10.1016/j.matpr.2016.09.020.

[18] J. Linke, T. Loewenhoff, V. Massaut, G. Pintsuk, G. Ritz, M. Rödig, A. Schmidt, C. Thomser, I. Uytdenhouwen, V. Vasechko, M. Wirtz, Performance of different tungsten grades under transient thermal loads, Nucl. Fusion. 51 (2011) 73017. doi:10.1088/0029-5515/51/7/073017.

[19] M. Wirtz, G. Cempura, J. Linke, G. Pintsuk, I. Uytdenhouwen, Thermal shock response of deformed and recrystallised tungsten, Fusion Eng. Des. 88 (2013) 1768–1772. doi:10.1016/j.fusengdes.2013.05.077.

[20] T. Loewenhoff, S. Bardin, H. Greuner, J. Linke, H. Maier, T.W. Morgan, G. Pintsuk, R.A. Pitts, B. Riccardi, G. De Temmerman, Impact of combined transient plasma/heat loads on tungsten performance below and above recrystallization temperature, Nucl. Fusion. 55 (2015) 123004. doi:10.1088/0029-5515/55/12/123004.

[21] H.S. Kim, S.T. Lim, Y. Jin, J.Y. Lee, J.M. Song, G.H. Kim, Recrystallization of bulk and plasma-coated tungsten with accumulated thermal energy relevant to Type-I ELM in ITER H-mode operation, J. Nucl. Mater. 463 (2015) 215–218. doi:10.1016/j.jnucmat.2014.12.002.

[22] S. Kanpara, S. Khirwadkar, S. Belsare, K. Bhope, R. Swamy, P. Mokariya, N. Patel, T. Patel, N. Chauhan, N. Jamnapara, Thermal shock behavior of Tungsten & Tungsten alloy materials under transient high heat load conditions, in: 10th Asia Plasma Fusion Assoc., Gandhinagar, India, 2015. doi:10.13140/RG.2.1.4664.6641.

[23] X. Liu, Y. Lian, L. Chen, Z. Chen, J. Chen, X. Duan, J. Fan, J. Song, Experimental and numerical simulations of ELM-like transient damage behaviors to different grade tungsten and tungsten alloys, J. Nucl. Mater. 463 (2015) 166–169. doi:10.1016/j.jnucmat.2014.12.114.

[24] Y. Lian, X. Liu, J. Wang, F. Feng, Y. Lv, J. Song, J. Chen, Influence of surface morphology and microstructure on performance of CVD tungsten coating under fusion transient thermal loads, Appl. Surf. Sci. 390 (2016) 167–174. doi:10.1016/j.apsusc.2016.08.060.

[25] T. Tanabe, V. Philipps, K. Nakamura, M. Fujine, M. Wada, B. Schweer, A. Pospieszczyk, B. Unterberg, Examination of material performance of W exposed to high heat load: Postmortem analysis of W exposed to TEXTOR plasma and E-beam test stand, J. Nucl. Mater. (1997) 241–243. doi:https://doi.org/10.1016/S0022-3115(97)80214-0.

[26] K. Nakamura, S. Suzuki, T. Tanabe, M. Dairaku, K. Yokoyama, M. Akiba, Disruption erosions of various kinds of tungsten, Fusion Eng. Des. 39 (1998) 295–301. doi:https://doi.org/10.1016/S0920-3796(98)00241-5.

[27] Y. Seki, K. Ezato, S. Suzuki, K. Yokoyama, H. Yamada, T. Hirayama, A study of plasma facing tungsten components with electrical discharge machined surface exposed to cyclic thermal loads, Fusion Eng. Des. 109–111 (2016) 1148–1152. doi:10.1016/j.fusengdes.2016.01.001.

[28] N. Klimov, V. Podkovyrov, A. Zhitlukhin, D. Kovalenko, J. Linke, G. Pintsuk, I. Landman, S.

Pestchanyi, B. Bazylev, G. Janeschitz, A. Loarte, M. Merola, T. Hirai, G. Federici, B. Riccardi, I. Mazul, R. Giniyatulin, L. Khimchenko, V. Koidan, Experimental study of PFCs erosion and eroded material deposition under ITER-like transient loads at the plasma gun facility QSPA-T, J. Nucl. Mater. 415 (2011) S59–S64. doi:10.1016/j.jnucmat.2011.01.013.

[29] V.P. Budaev, Y. V. Martynenko, A. V. Karpov, N.E. Belova, A.M. Zhitlukhin, N.S. Klimov, V.L. Podkovyrov, V.A. Barsuk, A.B. Putrik, A.D. Yaroshevskaya, R.N. Giniyatulin, V.M. Safronov, L.N. Khimchenko, Tungsten recrystallization and cracking under ITER-relevant heat loads, J. Nucl. Mater. 463 (2015) 237–240. doi:10.1016/j.jnucmat.2014.11.129.

[30] S. Lehto, J. Likonen, J.P. Coad, T. Ahlgren, D.E. Hole, M. Mayer, H. Maier, J. Kolehmainen, Tungsten coating on JET divertor tiles for erosion/deposition studies, Fusion Eng. Des. 66–68 (2003) 241–245. doi:10.1016/S0920-3796(03)00291-6.

[31] T.R. Barrett, G. Ellwood, G. Pérez, M. Kovari, M. Fursdon, F. Domptail, S. Kirk, S.C. McIntosh, S. Roberts, S. Zheng, L. V. Boccaccini, J.H. You, C. Bachmann, J. Reiser, M. Rieth, E. Visca, G. Mazzone, F. Arbeiter, P.K. Domalapally, Progress in the engineering design and assessment of the European DEMO first wall and divertor plasma facing components, Fusion Eng. Des. 109–111 (2016) 917–924. doi:10.1016/j.fusengdes.2016.01.052.

[32] C. Li, D. Zhu, X. Li, B. Wang, J. Chen, Thermal–stress analysis on the crack formation of tungsten during fusion relevant transient heat loads, Nucl. Mater. Energy. 13 (2017) 68–73. doi:10.1016/j.nme.2017.06.008.